

Dynamic Nuclear Polarization and Nuclear Magnetic Resonance in the Simplest Pseudospin Quantum Hall Ferromagnet

H. W. Liu^{1,*}, K. F. Yang², T. D. Mishima³, M. B. Santos³, and Y. Hirayama^{2,4,†}

¹*ERATO Nuclear Spin Electronics Project, Sendai, Miyagi 980-8578, Japan and State Key Lab of Superhard Materials and Institute of Atomic and Molecular Physics, Jilin University, Changchun 130012, P. R. China*

²*ERATO Nuclear Spin Electronics Project, Sendai, Miyagi 980-8578, Japan*

³*Homer L. Dodge Department of Physics and Astronomy, University of Oklahoma, Norman, OK 73019-2061, USA*

⁴*Department of Physics, Tohoku University, Sendai, Miyagi 980-8578, Japan*

*liuhw@ncspin.jst.go.jp

†hirayama@m.tains.tohoku.ac.jp

PACS numbers: 73.43.-f, 73.21.Fg, 73.63.Hs, 75.30.Kz

We characterize the simplest pseudospin quantum Hall ferromagnet with domain structures in single InSb quantum wells using resistively detected nuclear magnetic resonance (RDNMR). Dynamic nuclear polarization via the hyperfine interaction occurs when the domains with different pseudospin polarizations are energetically degenerate. The RDNMR signals of ¹¹⁵In are prominent, along with nine quadrupole splittings. The nuclear spin relaxation time T_1 is two orders of magnitude shorter than that of the bulk InSb, suggesting that collective spin excitations reside in the domain wall.

The study of magnetic properties in a two-dimensional electron gas (2DEG) is a powerful means to investigate the itinerant electron ferromagnetism (IEF) [1]. Rich physics is expected in this method involving tunable pseudospin (orbit, subband, and layer) degrees of freedom [2,3]. The simplest pseudospin quantum Hall ferromagnet (QHF) is formed at the filling factor [the number of occupied Landau levels (LLs)] of $\nu = 2$ in a monolayer 2DEG when the lowest two LLs with only orbital ($n = 0, 1$) and spin ($\sigma = \uparrow, \downarrow$) indices intersect using tilted magnetic fields [4]. The $\nu = 2$ QHF provides the ideal basis for a microscopic understanding of the domain formation, which is crucial for studying the IEF. Magnetotransport measurements in various 2DEGs have hitherto demonstrated either hysteretic or non-hysteretic longitudinal resistance spikes (or peaks) in the $\nu = 2$ QHF, presumably arising from the interplay between disorder and domain morphology analogous to that in conventional magnets [5-8]. So far, all experiments are limited to traditional transport measurements.

More recently, resistively detected NMR (RDNMR) was shown to be inherently sensitive to unveil novel spin phenomena in nano-scale and layered structures and study domains in a more complex QHF at fractional ν [9-17], which cannot be accomplished by other approaches. All RDNMR experiments have hitherto employed 2DEGs in GaAs, a host material in which electrons have a high electron mobility at low temperature and a small effective Lande g factor ($g^* \sim -0.44$). However, the small g^* makes it difficult to form the simplest pseudospin QHF using easily achievable fields.

In this Letter, we take advantage of the large g factors (over 50 in magnitude) of the typical narrow-gap semiconductor InSb to construct the simplest pseudospin QHF. Dynamic nuclear polarization (DNP) via the hyperfine interaction occurs when a large current flows through the QHF. The RDNMR signals of high nuclear spin isotopes of ^{115}In (nuclear spin $I = 9/2$), ^{123}Sb ($I = 7/2$), and ^{121}Sb ($I = 5/2$) are prominent, along with quadrupole splittings (QSs) of ^{115}In . The QS spectra exhibit diverse characteristics

in the $\nu = 2$ QHF, probably arising from the local strain at or near the domain wall where the DNP occurs. The fact that the nuclear spin relaxation time T_1 is about 120 s (almost temperature independent) is indicative of disordered spin-textured quasiparticles in the domain wall.

The 2DEG sample in this work is a Hall bar ($170 \times 40 \mu\text{m}$) fabricated using a symmetrically doped InSb quantum well [7]. This sample has a low-temperature electron mobility of $\mu = 14.3 \text{ m}^2/\text{Vs}$ and an electron density of $n_s = 1.83 \times 10^{15} \text{ m}^{-2}$. RDNMR and tilted-magnetic-field measurements were performed using a dilution refrigerator with an in-situ rotator. A low-frequency AC lock-in technique at 13.3 Hz was used to measure longitudinal resistances R_{xx} unless stated otherwise. The NMR was performed by a small CW RF field ($\sim \mu\text{T}$) generated by a single turn coil wound around the Hall bar.

The LL intersections are illustrated in the inset of Fig. 1 when tilting the 2DEG in a magnetic field B_{tot} . For simplicity, the field component B_{\perp} normal to the plane of the 2DEG (or the cyclotron energy between the neighboring LLs, $\hbar\omega_c = \hbar e B_{\perp} / m^*$, \hbar is the reduced Planck's constant) is kept constant. As the tilt angle θ increases, the Zeeman energy $\hbar\omega_s = g^* \mu_B B_{\text{tot}} = g^* \mu_B B_{\perp} / \cos\theta$ (μ_B is the Bohr magneton) increases and the LLs with different pseudospins (n, σ) intersect at integer ratios $r (= \hbar\omega_s / \hbar\omega_c = m^* g^* \mu_B / \hbar e \cos\theta)$. Because the InSb 2DEG has extremely large g^* with a magnitude of up to 70 [18], the ratio r is large, placing the LL degeneracy at experimentally accessible fields. This feature motivates the studies reported here.

Such an LL intersection can be mapped by peak positions of R_{xx} measured at different θ , as is shown in Fig.1 at a current of $I_{\text{sd}} = 3 \text{ nA}$. The LLs are widely separated at high fields because $\hbar\omega_c$ increases with increasing B_{\perp} . The LL intersections with small spin polarization $\zeta = r/\nu$ are characterized by a coalescence of R_{xx} (circle), while those with high ζ show resistance spikes within persistent R_{xx} minima (solid line). The resistance spike is suggestive of a domain formation [3]. For instance, the

pseudospin-down $[(n, \sigma) = (0, \downarrow)]$ and pseudospin-up $[(n, \sigma) = (1, \uparrow)]$ sublevels are brought to degeneracy at $\nu = 2$. First-order phase transition could occur from an unpolarized state $|(0, \uparrow), (0, \downarrow)\rangle$ to a fully polarized state $|(0, \uparrow), (1, \uparrow)\rangle$, showing easy-axis pseudospin anisotropy [2]. Disorder or finite temperature produces a domain wall separating domains with different spin polarizations [19]. Electron scattering between the neighboring LLs via the domain wall induces the resistance spike. Because the exchange energy E_{ex} is large at high ζ in the InSb 2DEG [18], the requirement of the domain formation is satisfied.

The dependence of R_{xx} on B_{\perp} around $\nu = 2$ at several angles is shown in Fig. 2(a). The resistance spike between two LL peaks seems to lie between $\theta = 57.4^{\circ}$ and $\theta = 62.2^{\circ}$. However, this angle range could be further extended by the RDNMR measurement. Figure 2(b) shows R_{xx} vs. B_{tot} over a range of I_{sd} . The spike amplitude R_{peak} is found to increase with I_{sd} , depending not only on electron transport across the Hall bar (see below) but also on heating effects. Figure 2(c) shows R_{peak} vs. temperature T and I_{sd} . The R_{peak} gives an estimate of the upper limit of the effective temperature T_e induced by I_{sd} . For instance, T_e is less than 1.5 K for $I_{\text{sd}} = 1.4 \mu\text{A}$ typically used in our RDNMR measurement.

We performed the RDNMR in the $\nu = 2$ QHF. As an example, we chose the resistance spike at $\theta = 59.5^{\circ}$ [Fig. 2(b)]. The measurement is initiated by sweeping B_{tot} to 7 T at $I_{\text{sd}} = 3 \text{ nA}$. Then, a large current of $1.4 \mu\text{A}$ is applied and time dependent R_{xx} is obtained [Fig. 3(a)]. When R_{xx} becomes saturated, the RF is set to irradiate the 2DEG while sweeping the frequency f through the Larmor resonance of individual nuclei. Figure 3(b) shows R_{xx} vs. f for ^{115}In . A dip featured in a resistance change ΔR_{xx} appears at resonance frequency $f_{\text{NMR}} = 65.42 \text{ MHz}$, representing an RDNMR signal. In a similar way, resonance signals of ^{121}Sb [Fig. 3(c)] and ^{123}Sb (data not shown) are also obtained. The f_{NMR} gives the gyromagnetic ratio $\gamma = 2\pi f_{\text{NMR}} / B_{\text{tot}}$: $\gamma_{^{115}\text{In}} = 58.7 \text{ MHz/T}$, $\gamma_{^{121}\text{Sb}} = 64 \text{ MHz/T}$, and $\gamma_{^{123}\text{Sb}} = 34.7 \text{ MHz/T}$, in accordance with those in the bulk InSb [20]. The RDNMR signal of ^{113}In is not observed due to its low

nuclear abundance (4.3%).

The RDNMR relies on the contact hyperfine interaction [21]. Because the energy for nuclear spin reversal is one-thousandth of that for electron spin reversal, electron-nuclear flip-flop requires a significant energy reduction in electron spin-flip. At the intersection around $\nu = 2$, the domains with different pseudospin polarizations are energetically degenerate, thereby allowing for the flip-flop. When a large current is applied, electrons move from one domain to the next and simultaneously polarize the relevant nuclei. Because the polarization only occurs at or near the domain wall with respect to electron spin-flip, the distributions of the DNP sites are inhomogeneous. This inhomogeneity induces additional domain disorder via the Overhauser shift [12], leading to extra dissipation between extended LL states and thus increasing R_{xx} . By contrast, the depolarization reduces the domain disorder and results in a decrease of R_{xx} [Figs. 3(b) and 3(c)]. Figure 3(d) shows the current dependent $\Delta R_{xx}/R_{xx}$ of ^{115}In , in which $\Delta R_{xx}/R_{xx}$ appears at $\sim 0.6 \mu\text{A}$ and increases with I_{sd} but decreases at higher I_{sd} as expected from current-induced heating effects. This plot is indicative of a current-dependent DNP.

The regions with detectable RDNMR in the $\nu = 2$ QHF are mapped in Fig. 2(a) (dots and dashed curves). Apparently, the DNP always follows the resistance spike. More interestingly, the high-sensitivity RDNMR allows us to probe the spike hidden in the LL peak and thereby determine the real borders of the $\nu = 2$ QHF between $\theta = 53.2^\circ$ and $\theta = 64.3^\circ$.

Further reducing the RF sweep rate enables us to resolve the QSs of ^{115}In [Figs. 4(a) and 4(b)]. The fit in Fig. 4(b), as indicated by a red line composed of nine nearly equally spaced Gaussian curves, is in good agreement with the data. These nine curves are responsible for resonant transitions among ten quadrupole levels of ^{115}In with equal intervals [22]. In the case of uniaxial strain along the growth direction, the splitting frequency of $\sim 57 \text{ kHz}$ [Fig. 4(b)] gives an estimate of deformation tensor element $e_{zz} \sim 0.2\%$,

indicating less strain at relevant nuclear positions [23]. This in principle coincides with our expectation that the lattice mismatch in the InSb QW is small ($\sim 0.7\%$). However, the strain analyses in the QHF are found to be complicated. The QSs exhibit different fine structures in the $\nu=2$ QHF, as is shown in Fig. 4. We suppose that such diverse properties arise from the local strain at or near the domain wall where the DNP occurs, associated with the morphology, size, fluidity, and spatial distribution of the domains. Further studies of the strain in the QHF are expected to promote understanding of the domain formation. Note that we do not take the Knight shift into account in the above analysis because the Knight shift in InSb [24] is smaller than the measured QS.

The procedure for measuring T_1 is shown in the inset of Fig. 5. The solid line is a fit to a single exponential used to determine T_1 [16]. Figure 5 shows T_1 vs. I_{sd} , in which T_1 does not exhibit notable current dependence. Because the large current could heat the sample, the data also suggest that T_1 is almost temperature-independent. This is consistent with the observation in the ferromagnetic state of GaAs 2DEGs [14,16]. The average T_1 of 120 s, about two orders of magnitude shorter than that in the bulk InSb [21], indicates that collective spin excitations responsible for significantly enhanced nuclear spin relaxation [25] may reside in the domain wall. The T_1 is probably limited by spin-textured quasipariteles induced by disorder and thereby shows T -independent. It is worth noting that the spin-orbit (SO) interaction played a role in T_1 [26]. The Rashba SO was neglected in symmetrically doped InSb 2DEG [7]. The Dresselhaus SO (usually large in narrow-gap semiconductors), however, may contribute to the reduced T_1 to some extent via the spin mixing. Further experiments are needed to reveal its role. In addition, T_1 is found to be almost constant at all spikes around $\nu=2$ except that it reaches up to 500 s at the border spike at $\theta = 53.2^\circ$. At this point, we do not yet know the mechanism.

We further probed the DNP at the resistance spikes around $\nu=3$ and $\nu=4$ (Fig. 1), but no RDNMR

was observed. This is different from the observations at fractional ν where the RDNMR is observed in the QHFs around filling factors $\nu^* = 2, 3$ and 4 of composite Fermions (CFs) [12]. Note that the QHFs at fractional ν occur at high B_{\perp} for a large ν^* of the CFs, while those in the IQHE are at low B_{\perp} for a large ν . At low B_{\perp} (corresponding to a large magnetic length $\ell_B \sim \sqrt{1/B_{\perp}}$), the domain size is expected to be large. Therefore, the number of domains participating in electron spin-flip decreases, which might account for the disappearance of the RDNMR. In addition, no RDNMR signals are observed at the LL intersections marked with circles in Fig. 1. Measurements of g^* in the InSb 2DEG suggest that the exchange interaction induces a large gap at these intersections [18]. However, the exchange energy is not strong enough to form the domain. Because of this large energy gap, we proved that the thermal- or breakdown-induced nuclear polarization accessible in the GaAs QWs [27,28] could not be implemented at or near these intersections.

In conclusion, we systematically probed the LL intersections in the InSb 2DEG using RDNMR. Domain structures are found to be required for the DNP at the LL intersection. The demonstration of the DNP in the simplest pseudospin QHF makes it possible to study domains by virtue of the T_1 measurement and QS spectra. This enables fundamental studies towards a microscopic understanding of the domain formation associated with the hyperfine coupling, exchange interaction, SO coupling, and local strain. Clear observations on the Qs of ^{115}In support the possibility to coherently control the ten nuclear-spin quantum levels and build multiple NMR-based quantum bits (≥ 2). Our experiments also offer unique opportunities to investigate spin phenomena in quantum structures made of narrow-gap semiconductors, which will promote these materials as candidates in the emerging field of spintronics.

We acknowledge helpful discussions with K. Hashimoto and N. Shibata in Tohoku University, S. Watanabe in ERATO-JST, and K. Muraki in NTT-BRL. H.W.L. thanks the Program for New Century Excellent Talents of University in China.

References

- [1] E. P. De Poortere *et al.*, Science **290**, 1546 (2000).
- [2] T. Jungwirth and A. H. MacDonald, Phys. Rev. B **63**, 035305 (2000).
- [3] T. Jungwirth and A. H. MacDonald, Phys. Rev. Lett. **87**, 216801 (2001).
- [4] R. J. Nicholas *et al.*, Phys. Rev. B **37**, 1294 (1988).
- [5] J. Jaroszyński *et al.*, Phys. Rev. Lett. **89**, 266802 (2002).
- [6] G. M. Gusev *et al.*, Phys. Rev. B **67**, 155313 (2003).
- [7] J. C. Chokomakoua *et al.*, Phys. Rev. B **69**, 235315 (2004).
- [8] K. Vakili *et al.*, Phys. Rev. Lett. **94**, 176402 (2005).
- [9] S. Kronmüller *et al.*, Phys. Rev. Lett. **82**, 4070 (1999).
- [10] J. H. Smet *et al.*, Nature **415**, 281 (2002).
- [11] K. Hashimoto *et al.*, Phys. Rev. Lett. **88**, 176601 (2002).
- [12] O. Stern *et al.*, Phys. Rev. B **70**, 075318 (2004).
- [13] G. Yusa *et al.*, Nature **434**, 1001 (2005).
- [14] N. Kumada, K. Muraki, and Y. Hirayama, Science **313**, 329 (2006).
- [15] L. A. Tracy *et al.*, Phys. Rev. Lett. **98**, 086801 (2007).
- [16] X. C. Zhang, G. D. Scott, and H. W. Jiang, Phys. Rev. Lett. **98**, 246802 (2007).
- [17] N. Kumada, K. Muraki, and Y. Hirayama, Phys. Rev. Lett. **99**, 076805 (2007).
- [18] B. Nedniyom *et al.*, Phys. Rev. B **80**, 125328 (2009).
- [19] L. Brey and C. Tejedor, Phys. Rev. B **66**, R041308 (2002).
- [20] W. G. Clark and G. Feher, Phys. Rev. Lett. **10**, 134 (1963).
- [21] M. Gueron, Phys. Rev. **135**, A200 (1964).
- [22] R. K. Sundfors, Phys. Rev. **185**, 458 (1969).

[23] R. I. Dzhioev and V. L. Korenev, Phys. Rev. Lett. **99**, 037401 (2007).

[24] D. P. Tunstall, J. Phys. C **21**, 2853 (1988).

[25] R. Côté *et al.*, Phys. Rev. Lett. **78**, 4825 (1997).

[26] K. Hashimoto *et al.*, Phys. Rev. Lett. **94**, 146601 (2005).

[27] W. Desrat *et al.*, Phys. Rev. Lett. **88**, 256807 (2002).

[28] M. Kawamura *et al.*, Appl. Phys. Lett. **90**, 022102 (2007).

FIG. 1 (color online). Peak positions of longitudinal resistance R_{xx} vs. perpendicular field B_{\perp} (or ν) and $1/\cos\theta$ at $I_{sd} = 3$ nA and $T = 200$ mK. The dashed line denotes the LL intersections at the same coincidence ratio r . Left inset shows a schematic plot of the LL evolution at constant B_{\perp} (or $\hbar\omega_c$) for the 2DEG in tilted fields (right inset). Indices (n, σ) label relevant pseudospin levels and integer numbers denote ν .

FIG. 2 (color online). (a) R_{xx} as a function of B_{\perp} at several angles. The curves are offset for clarity. Dots together with the dashed curves around resistance spikes map the RDNMR region. The dot diameter denotes the ratio between the DNP-induced resistance change ΔR_{xx} and R_{xx} of ^{115}In . (b) R_{xx} vs. B_{tot} at different I_{sd} with constant intervals of 0.25 μA at $\theta = 59.5^\circ$. (c) Peak height R_{peak} of the spikes in (b) vs. temperature T and I_{sd} . The solid line is a fit following $\exp(-\sqrt{T_0/T})$ behavior with $T_0 = 25.6$ K, suggestive of a hopping transport at the LL intersection [7].

FIG. 3. (a) Time dependence of R_{xx} at $\theta = 59.5^\circ$, $B_{tot} = 7$ T, and $T = 100$ mK after I_{sd} changes from 3 nA to 1.4 μA . (b) RDNMR signal of ^{115}In at an RF sweep rate of 20 kHz/min. (c) RDNMR signal of ^{121}Sb obtained using an AC resistance bridge with a current of 1 μA at 60 kHz/min. (d) $\Delta R_{xx}/R_{xx}$ of ^{115}In as a function of I_{sd} .

FIG. 4 (color). (a to d) RDNMR signals of ^{115}In at a slow RF sweep rate of 3 kHz/min and $T = 100$ mK. The red line in (b) is a fit with nine Gaussian curves (green color). Note that a hump rather than a dip is observed in (b) and (d). These two data are obtained from the spikes hidden in broad LL peaks. In this case, the polarized spike might shift relative to the unpolarized spike, with the result that R_{xx} in one flank of the polarized spike is smaller than that of the unpolarized spike, accounting for the hump feature.

FIG. 5. Nuclear spin relaxation time T_1 of ^{115}In as a function of I_{sd} at $\theta = 59.5^\circ$, $B_{tot} = 7$ T, and $T = 100$ mK. The inset shows the measurement of T_1 by recording the time evolution of R_{xx} with on-resonance (65.43 MHz) and off-resonance RF irradiation.

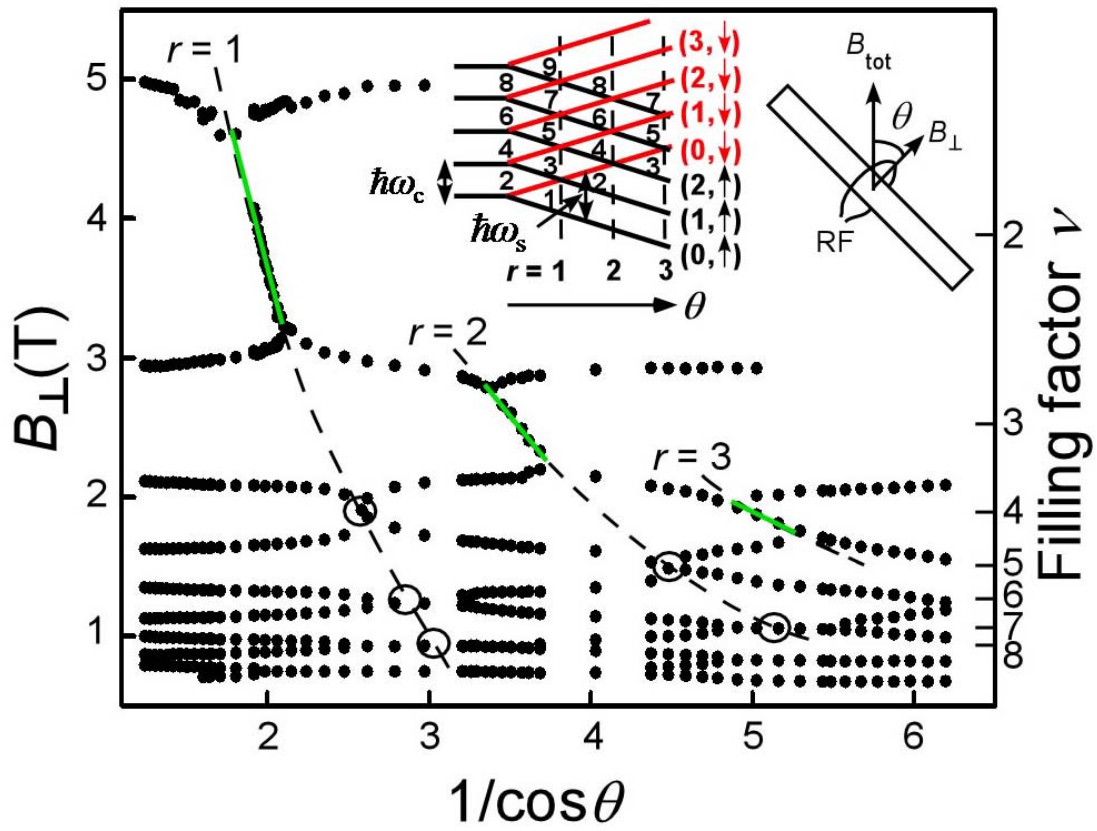


FIG.1

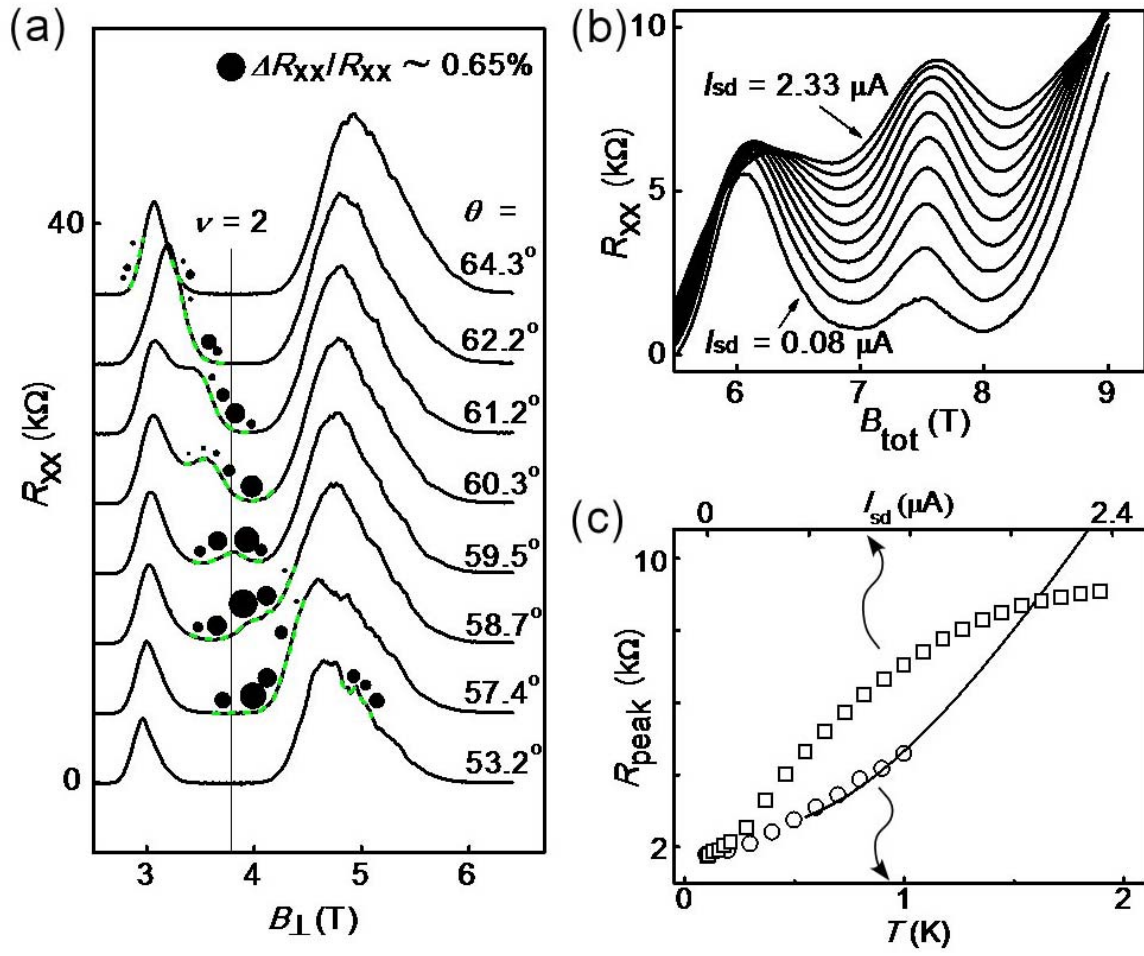


FIG. 2

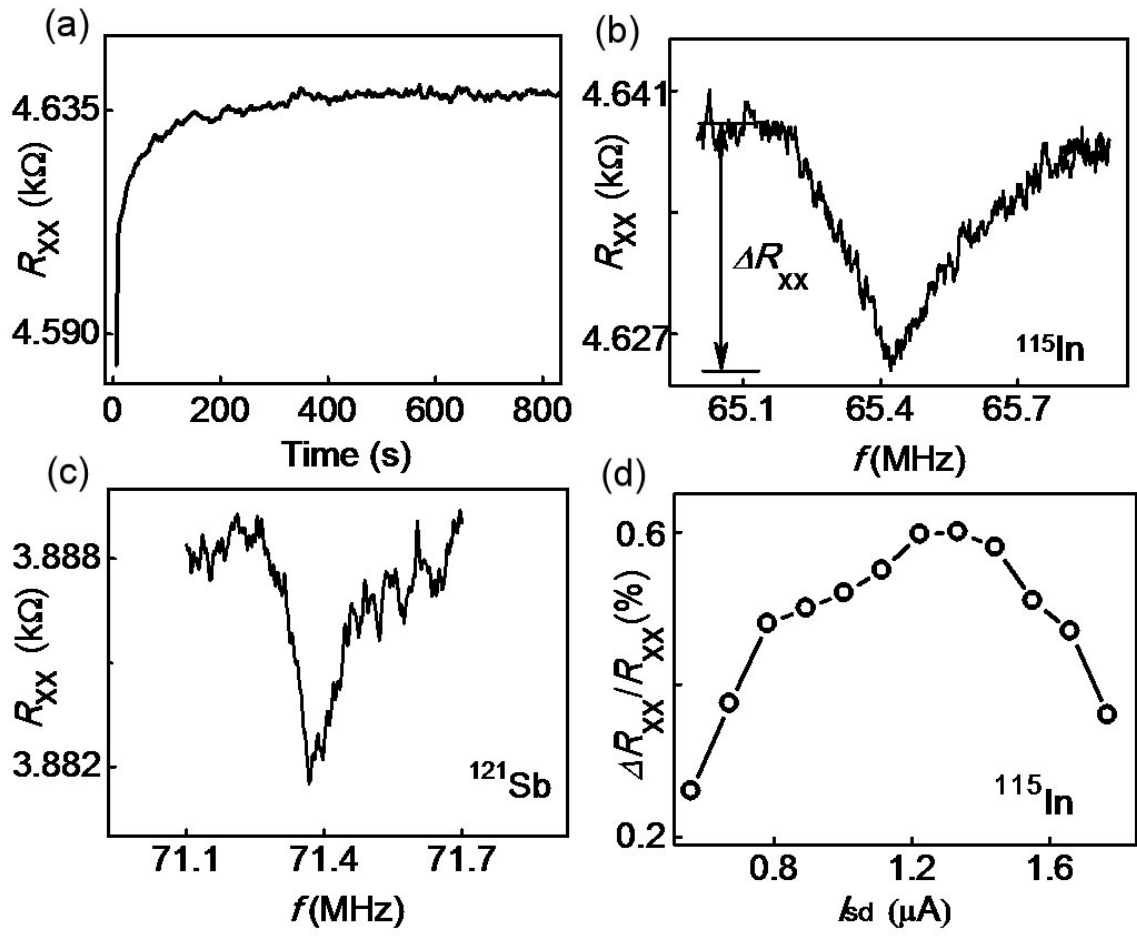


FIG. 3

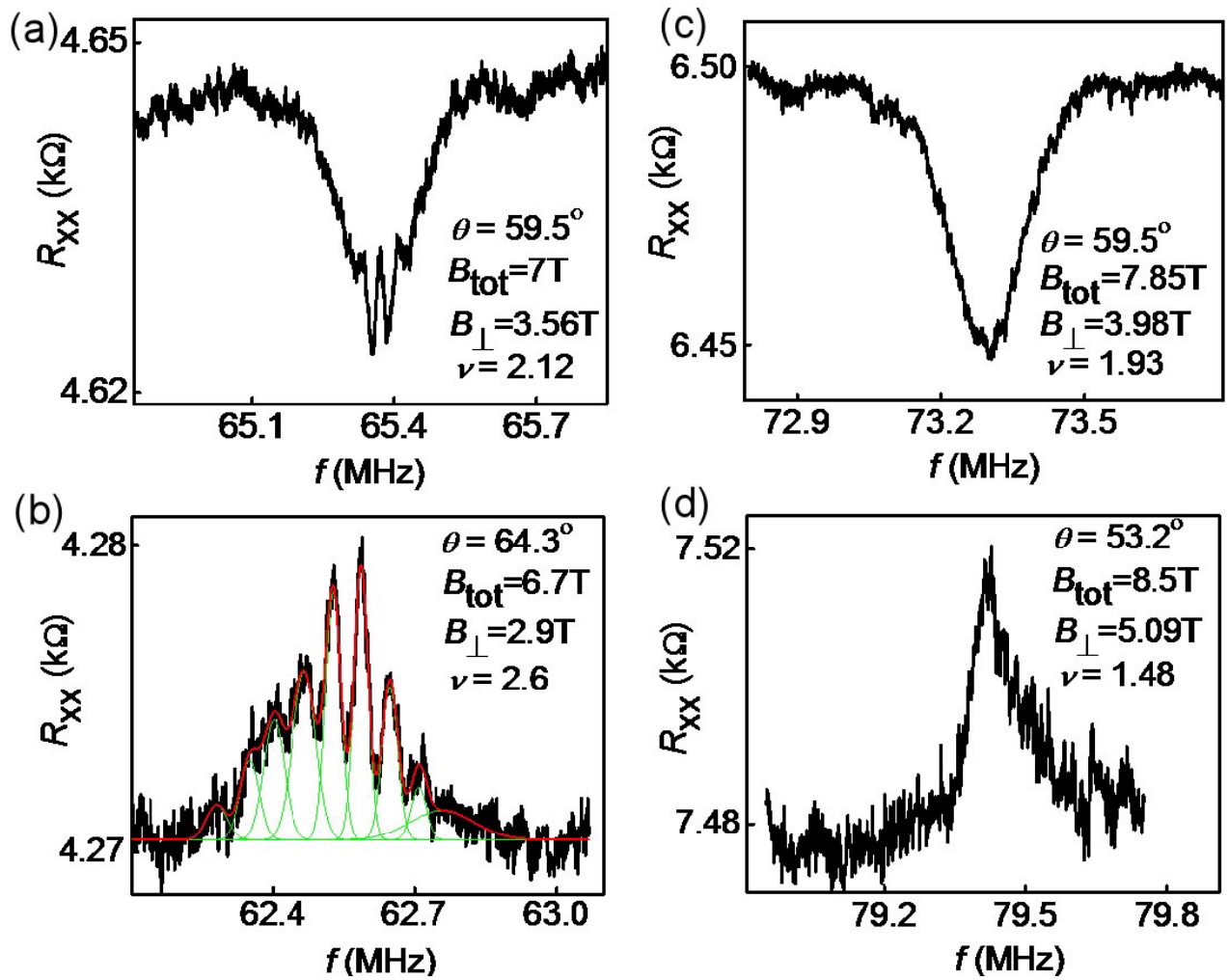


FIG. 4

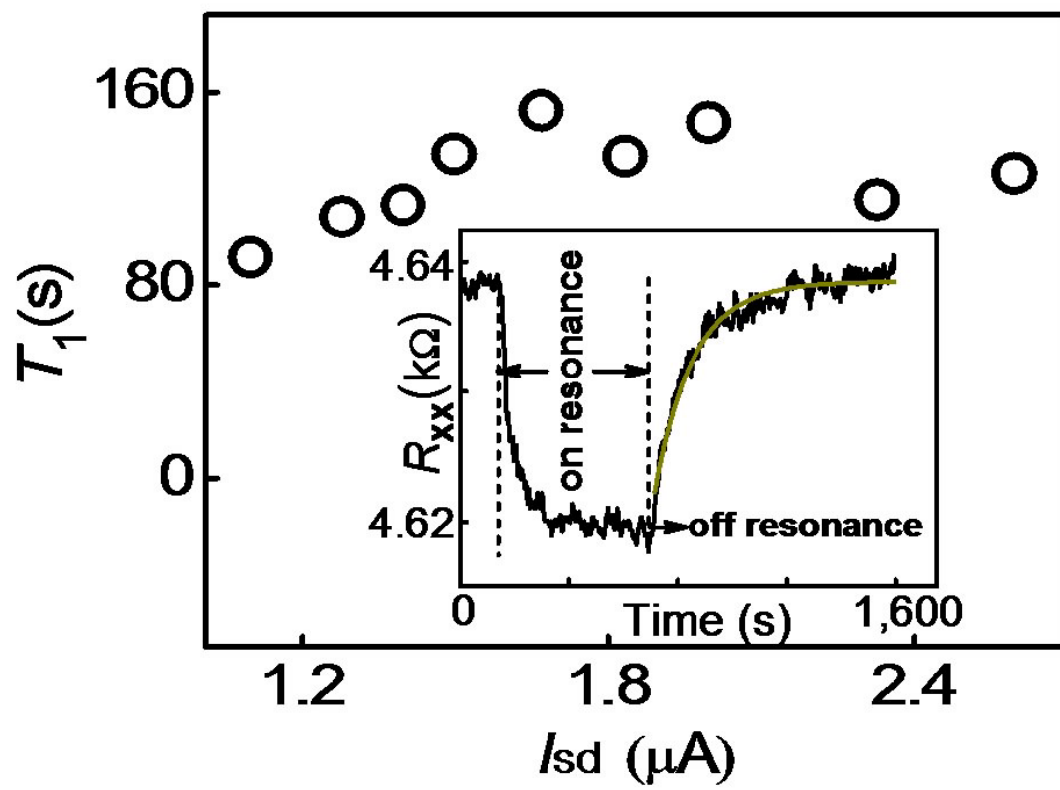


FIG. 5